Modeling of Stresses at Grain Boundaries with Respect to Occurrence of Stress Corrosion Cracking

K. J. Kozaczek [1], A. Sinharoy [2], C. O. Ruud [2], and A. R. McIlree [3]

ABSTRACT

The distributions of elastic stresses/strains in the grain boundary regions were studied by the analytical and the finite element models. The grain boundaries represent the sites where stress concentration occurs as a result of discontinuity of elastic properties across the grain boundary and the presence of second phase particles elastically different from the surrounding matrix grains. A quantitative analysis of those stresses for steels and nickel based alloys showed that the stress concentrations in the grain boundary regions are high enough to cause a local microplastic deformation even when the material is in the macroscopic elastic regime. The stress redistribution as a result of such a plastic deformation was discussed.

KEY WORDS: stress, strain, grain boundaries, carbide precipitates, stress corrosion cracking.

INTRODUCTION

The presence of stresses (applied, residual or a combination thereof) is one of the conditions for stress corrosion cracking to occur. The general perception is that the presence of tensile stresses promotes crack initiation and accelerates its propagation. The postulated mechanisms explain the role of stresses in terms of purely mechanical concepts (local stress concentration at material discontinuities, localized plastic deformation) or in terms of stress assisted phenomena such as slip-dissolution and hydrogen-induced cracking. In the case of intergranular stress corrosion cracking grain boundaries play an essential role since they represent a discontinuity of the physical, chemical and mechanical properties in otherwise homogeneous material. From the mechanics point of view grain boundaries represent the sites where stress concentration occurs as a result of discontinuity of elastic properties across the grain boundary, presence of second phase particles elastically different from the surrounding matrix grains, and higher density of lattice defects than the grain interiors. The following sections will present some modeling approaches to the first two aforementioned classes of site conditions.

DISTRIBUTION OF STRESSES AND STRAINS IN POLYCRYSTALS

Effect of Elastic Anisotropy and the Shape of Grains

Single crystals (grains) are elastically anisotropic. For most structural materials such as steels and nickel based alloys, which have a cubic crystal structure, this anisotropy can be described by the Zener anisotropy factor, A, defined as:

[1] Oak Ridge National Laboratory, Oak Ridge, Tennessee, USA.
[2] The Pennsylvania State University, University Park, Pennsylvania, USA.
[3] Electric Power Research Institute, Palo Alto, California, USA.

$$A = 2C_{44}/(C_{11}-C_{12}) \quad (1)$$

where C_{44} and $(C_{11}-C_{12})/2$ represent the shear resistance in a [100] direction on a (100) plane and in a [110] direction on a (110) plane, respectively. For perfectly isotropic crystals A=1, for nickel and nickel superalloys A≈2.70-2.80. A single phase polycrystal is an aggregate of randomly oriented crystallites (grains). The macroscopic, long range stress is distributed between the individual grains and the stress in a particular grain depends on the grain orientation with respect to the applied stress, and its interactions with the neighboring grains. In general, the grain to grain interactions in a polycrystalline aggregate depend on the grain size distribution, grain boundary misorientation distribution, and Zener anisotropy factor. The higher the anisotropy factor the larger is the scatter in observed stresses.[1] Dikusar *et al.*[2] used the theory of random functions to analyze the microdeformation of random polycrystals. The model polycrystal was composed of the uniform size grains and the inhomogeneity of the material resulted from the presence of definite boundaries between the separate crystallites. Assuming a normal distribution density of the grains with respect to the stress, i.e., assuming that almost all (i.e., 99.7%) possible values of stress lie in the interval $\sigma \pm 3$ S, where σ is the external stress averaged over all crystallites and S is the standard deviation proportional to stress:

$$S = \sigma \cdot \Delta \quad (2)$$

$$\Delta = 0.145 \cdot K \cdot |\lambda| / (K+4/3G) \cdot E \quad (3)$$

where: K is the bulk modulus; G is the shear modulus; E is Young's modulus, and $\lambda = C_{11} - C_{12} - 2C_{44}$; C_{ij} are single crystal elastic constants. The term $(1+3\Delta)$ represents the stress concentration factor due to the discontinuity of elastic properties across the grain boundary, and for nickel alloys is equal to 1.2; higher values of stress concentration can occur but with low probability i.e., 0.3% of grains are subjected to stresses higher than 1.2σ.

Additional stress concentrations at grain boundaries stem from the fact that the grain size distribution in real polycrystalline materials is not uniform but best approximated by the gamma distribution or two-parameter lognormal distribution.[3-5] As a result, grains with different sizes have different number of neighbors, and the resultant interaction stresses are different. The stress distributions in a fully dense aggregate composed of grains having a lognormal size distribution have been studied by a finite element model.[6] A 3-dimensional microstructure was simulated using a Voronoi-Poisson tessellation generated within a unit cube (Figure 1). The simulated microstructure contained 500 grains and was shown to be topologically correct[3]. Each grain was divided into tetrahedral elements having a common vertex at the location of the original seed from which the grain had been grown. Such a division provided for 40-50 finite elements per grain. The simulated microstructure had a random orientation of grains i.e., no crystallographic texture. Recognizing that a stress corrosion crack initiates at the surface where a plane state of stress is present, a biaxial pressure uniformly distributed on the cube faces was applied (Figure 1). The two unloaded surfaces remained free. Two scalar stresses were calculated at the vertices where the grains meet (4 grains meet at a common vertex in the bulk material, 3 grains meet at the surface): von Mises stress (second invariant of the deviator stress tensor) as relevant to the slip-type mechanism of crack initiation, and hydrostatic stress (one third of the first invariant of the stress tensor) as relevant to the hydrogen embrittlement type of material damage. An example of stress distributions on a surface is shown in Figure 2. From Figure 2 it is evident that the microstructural features, such as small grains, or rather a small cross-section of a grain with the surface (for example the grain marked as A) with sharp shapes, act as stress raisers, regardless of their own orientation and the orientations of the adjacent grains. The computer simulations showed that the grain size, shape, and orientation had a more pronounced effect on stress distribution than the loading conditions (i.e., uniaxial vs. biaxial loading). For Alloy 600, the stress concentration at grain boundary vertices was found to be 1.7 for the hydrostatic pressure and 1.5 for the von Mises stresses.

The distribution of elastic stresses and strains in the grain interiors (between grain portions represented by finite elements) was found to be a normal (Gaussian) distribution. Figure 3 shows the distribution of the hydrostatic and von Mises strains. The strain/stress distributions on cube surfaces and in the cube interior are very similar showing that there is no surface effect on the elastic

stress/strain distribution. The mean value of stresses/strains (0 in units of standard deviation as shown in Figure 3) corresponds approximately to the value of the applied macroscopic stress. The standard deviation S depends on the elastic anisotropy of the material[1,2]; the higher the elastic anisotropy (i.e., the more the Zener factor deviates from A=1) the higher the standard deviation. For Alloy 600 (Zener anisotropy factor A=2.76) the standard deviation of von Mises stress was found to be 25% of the applied stress and for hydrostatic pressure the standard deviation was 40% of the applied stress. Therefore, from the properties of a normal distribution, it follows that 68% of the material volume is subjected to the stress $\sigma \pm S$ (σ is the mean applied stress), 99.7% of the volume is subjected to $\sigma \pm 3S$ *etc.* In terms of the extreme values of stress, 0.3% of the material (grains) is subjected to stress 2.2 (or more) times higher than the applied hydrostatic stress and 1.75 (or more) times higher than the applied von Mises stress. These results, compared with the analysis for uniform grain size[2] show that the grain size distribution, other than uniform, is responsible for increased interaction stresses between grains and, therefore, for higher maximum stresses.

Effect of Second Phase Particles

The previous section discussed the stress/strain distribution in the grain boundary regions of a single phase alloy. The presence of second phase particles (carbide precipitates) at grain boundaries changes the stress field since the carbides have different elastic properties than the alloy grains. The residual stresses resulting from the mismatch of the thermo-expansion coefficients of the matrix and the precipitates are not considered in this analysis. The single crystal elastic constants and thermal expansion coefficients for most common M_7C_3 and $M_{23}C_6$ carbides are not available. In general, however, the precipitates have a higher stiffness than the metal matrix. Figure 4 shows a model of a second-phase particle (with the Young's modulus twice that of the matrix material) at the grain boundary triple point.[7,8] The model satisfies the carbide-matrix orientation relationship and also provides for the maximum elastic mismatch between the grains. When the system is loaded in the uniaxial mode (Figure 4) the hydrostatic pressure in the matrix shows a variation from tensile to compressive with a stress concentration factor of K_c=1.97 and the ratio of the maximum to minimum stresses $\sigma_{max}/\sigma_{min}$=-15.5. A stress field of the size approximately that of the precipitate is aligned with the direction of the applied load and the maximum stresses occur at the precipitate/matrix interface. The stress concentration factor for the von Mises stress in the matrix is K_c=1.67. The von Mises stress variation in the matrix is $\sigma_{max}/\sigma_{min}$=3.65. The stress concentration factors are higher than those presented in the previous section for a single phase material with "clean" grain boundaries. The difference between those two cases represents the effect of carbides on stress distribution in grain boundary regions. A significant difference, aside from increasing the magnitude of maximum stresses, is that hydrostatic stresses can have a sign opposite to that of the applied load i.e., applied compressive stresses can result in tensile hydrostatic stresses around precipitates.

Stress Redistribution Due to Local Plastic Deformation

Since the elastic stresses are highest in the vicinity of carbide precipitates, the most likely scenario is that local microplastic deformation (even if the polycrystal is in the macroscopic elastic regime, below the macroscopic yield strength) will start in those regions. Indeed, experimental evidence shows that dislocation loops are punched out at incoherent interfaces and misfit dislocations are generated along semi-coherent interfaces.[9] Such a microplastic deformation causes a redistribution of elastic stresses in the grain boundary regions. The redistribution of stresses due to slip or a narrow shear band formation was studied by a finite element method.[10] The grains, shown in Figure 5, were misoriented by 45 degrees with respect to each other and had the elastic properties of Alloy 600 single crystals; the carbide precipitate was twice as stiff as the matrix. The grain boundary is shown as a vertical line, the slip band is the horizontal line in the left side grain. Figure 5(a) shows the normal stress fields before the deformation took place, Figure 5(b) shows the redistributed stresses. The plastic deformation reduces the shear stresses in the vicinity of a carbide, but causes a substantial increase of normal stresses. The normal stresses which tend to separate the matrix from the carbide increased to a value 5 times higher than the applied shear stresses as a result of the local plastic deformation.[10] With such a high increase of normal stresses across the carbide/matrix interface, the possibility of debonding should be considered.

CONCLUSIONS

The distributions of elastic stresses and strains in the grain boundary regions were studied by the analytical and finite element models. The grain boundaries represent the sites where stress concentration occurs as a result of discontinuity of elastic properties across the grain boundary and the presence of second phase particles elastically different from the surrounding grains of a matrix. A quantitative analysis of those stresses for steels and nickel based alloys showed that the stress concentrations in the grain boundary regions are high enough to cause a local microplastic deformation even when the material is in the macroscopic elastic regime. The stress redistribution as a result of such a plastic deformation was discussed.

ACKNOWLEDGMENTS

Research sponsored by the Electric Power Research Institute, Palo Alto, CA under contract RP2812-13. One of the authors (KJK) was partially sponsored by the U. S. Department of Energy, Assistant Secretary for Energy Efficiency and Renewable Energy, Office of Transportation Technologies, as part of the High Temperature Materials Laboratory User Program under contract DE-AC05-84OR21400, managed by Lockheed Martin Energy Systems.

REFERENCES

1. S.Kumar, S.K. Kurtz, and V.K. Agarwala, Acta Mechanica 108 (1995): p. 1.
2. L.D. Dikusar, E.F. Dudarev, and V.E. Panin, Izv. Vyssh. Uchebn. Zaved., Fizika 8 (August 1971): p. 96.
3. S. Kumar, S.K. Kurtz, J.R. Banavar, and M.G. Sharma, J. Stat. Physics 67, 3/4 (May 1992): p. 523.
4. S.K. Kurtz, F.M.A. Carpay, J. Appl. Phys. 51, 11 (Nov. 1980): p. 5725.
5. S.K. Kurtz, F.M.A. Carpay, J. Appl. Phys. 51, 11 (Nov. 1980): p. 5745.
6. K.J. Kozaczek, B.G. Pertovic, C.O. Ruud, and S.K. Kurtz, J. Materials Science 30 (1995): p. 2390.
7. K.J. Kozaczek, A. Sinharoy, C.O. Ruud, and A.R. McIlree, Modeling and Simulation in Materials Science and Engineering, in press.
8. K.J. Kozaczek, A. Sinharoy, C.O. Ruud, and A.R. McIlree, "Modeling of Grain Boundary Stresses in Alloy 600," in Fatigue and Crack Growth: Environmental Effects, Modeling Studies, and Design Considerations, PVP-Vol. 306, ed. S. Yukawa (New York, NY: ASME, 1995), p. 213.
9. S.M. Bruemmer, in EPRI Alloy 600 Expert Meeting, Airlie, VA, 1993, ed. A.R. McIlree (Palo Alto, CA:EPRI, in press).
10. K.J. Kozaczek, C.O. Ruud, EPRI Report, in preparation.

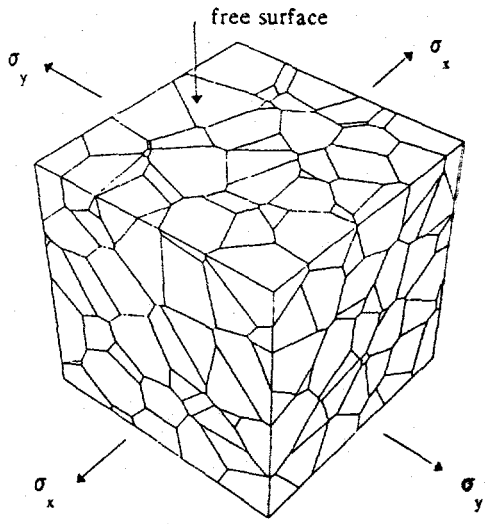

Figure 1. *Simulation of a three-dimensional microstructure of a single phase alloy. After [6].*

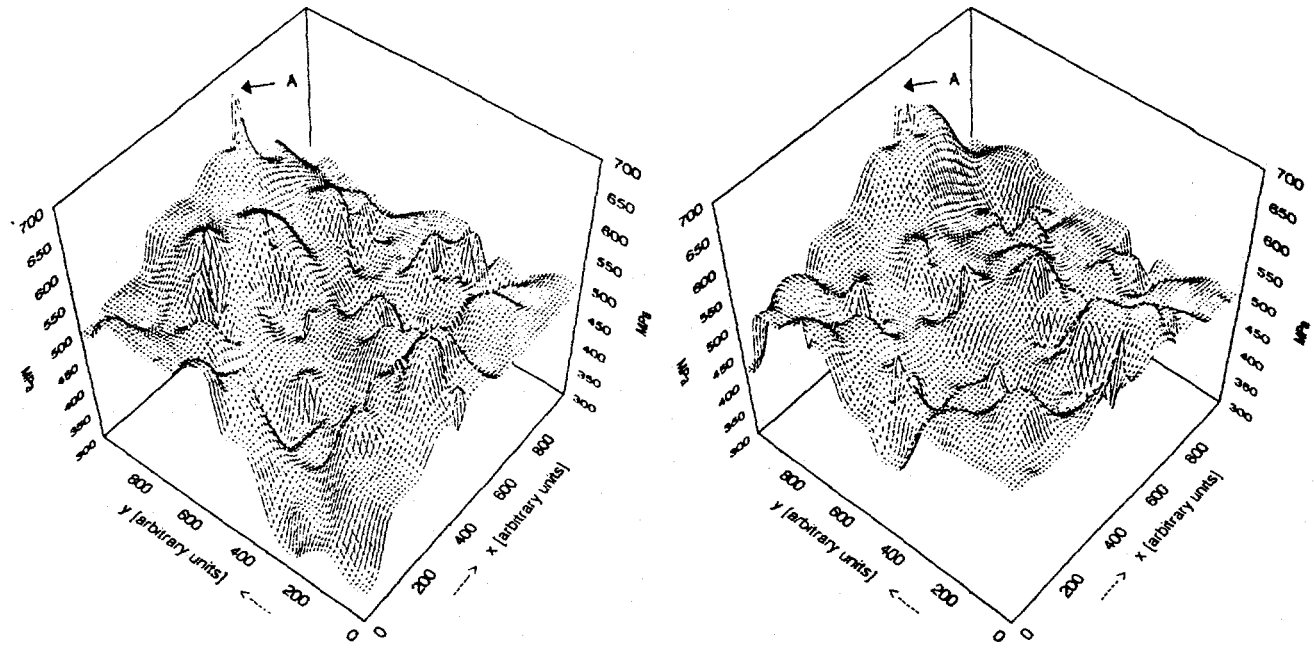

(a) (b)

Figure 2. Distribution of von Mises stresses on the free surface, simulation of 500 grains. Loading conditions: (a) σ_x = 500 MPa, σ_y =-10 MPa, (b) σ_x = 300 MPa, σ_y = -300 MPa. After reference [6].

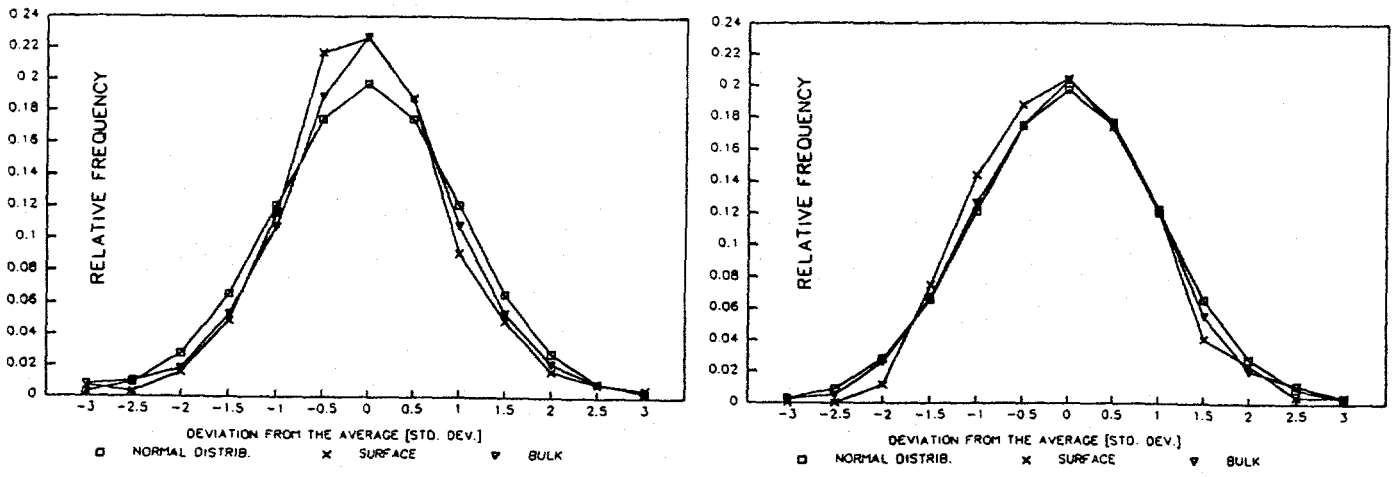

(a) (b)

Figure 3. Distribution of hydrostatic strains (a) and von Mises strains (b) on the surface and in the bulk of Alloy 600.

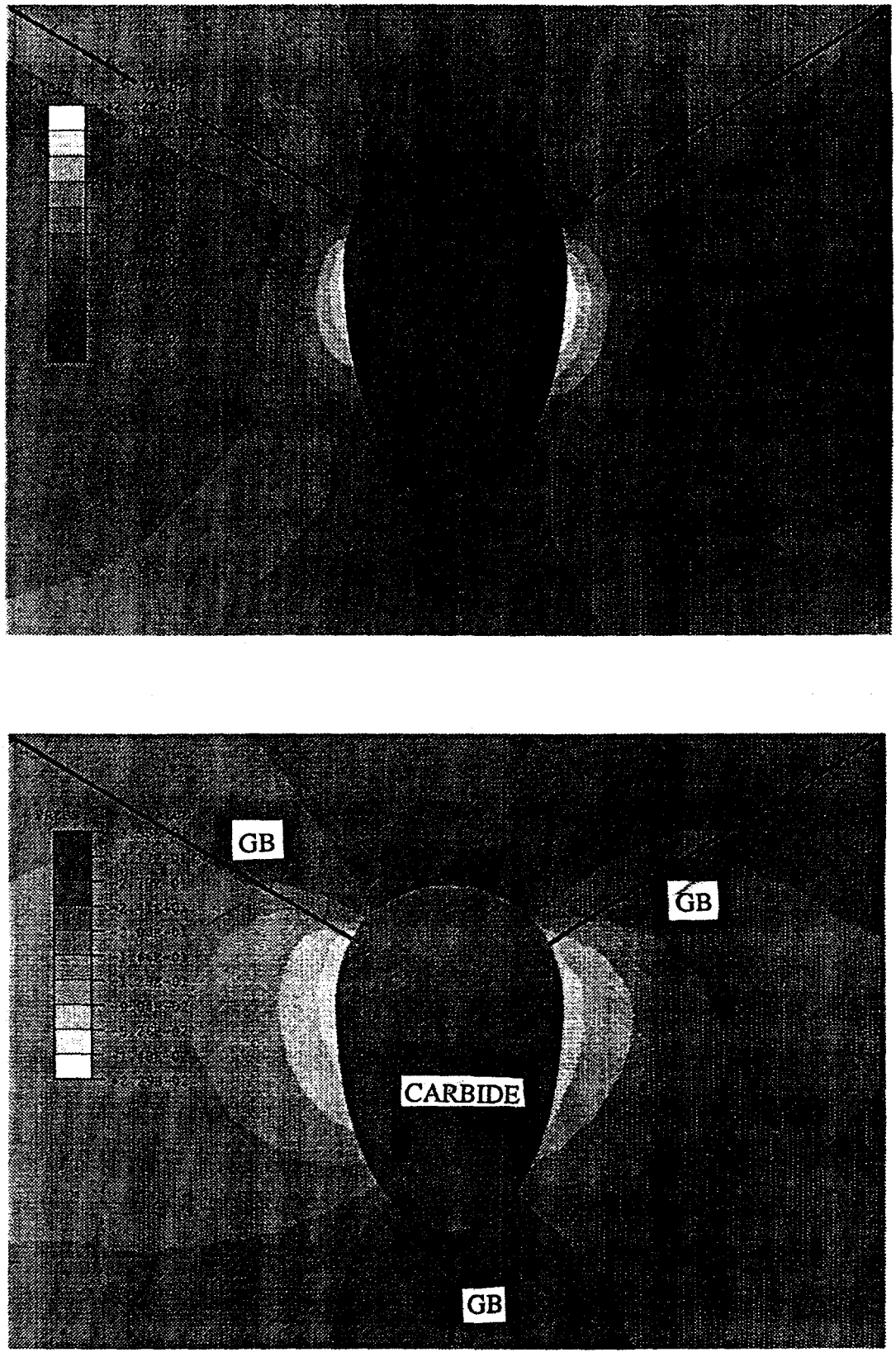

Figure 4. Von Mises stress (a) and hydrostatic pressure (b) around a carbide precipitate at a grain boundary (GB) due to uniaxial tension. Stresses in MPa. After reference [6].

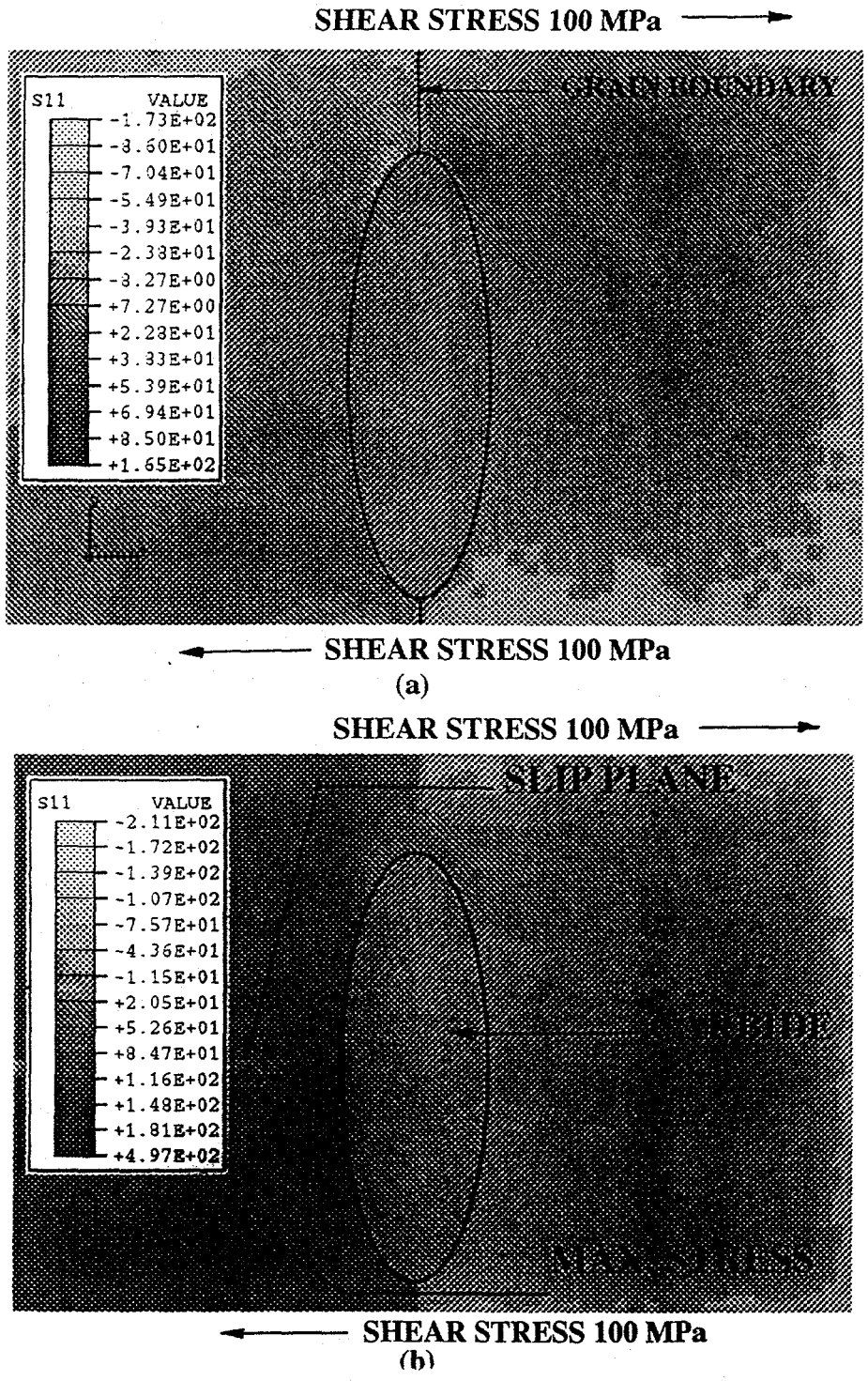

Figure 5. Distribution on normal stresses (a) before deformation and (b) as a result of microplastic deformation. Stresses in MPa.

DISCLAIMER